frontiers in Plant Science

ORIGINAL RESEARCH
published: 14 August 2020
doi: 10.3389/fpls.2020.01248

Stomatal Sensitivity to Vapor Pressure Deficit and the Loss of Hydraulic Conductivity Are Coordinated in *Populus euphratica*, a Desert Phreatophyte Species

Da-Yong Fan[1], Qing-Lai Dang[2], Cheng-Yang Xu[1], Chuang-Dao Jiang[3], Wang-Feng Zhang[4], Xin-Wu Xu[3,5], Xiao-Fang Yang[3] and Shou-Ren Zhang[3]**

[1] College of Forestry, Beijing Forestry University, Beijing, China, [2] Faculty of Natural Resources Management, Lakehead University, Thunder Bay, ON, Canada, [3] State Key Laboratory of Vegetation and Environmental Change, Institute of Botany, The Chinese Academy of Sciences, Beijing, China, [4] The Key Laboratory of Oasis Eco-agriculture, Xinjiang Production and Construction Corps, Shihezi University, Shihezi, China, [5] China Meteorological Administration, Beijing, China

OPEN ACCESS

Edited by:
Virginia Hernandez-Santana, Institute of Natural Resources and Agrobiology of Seville (CSIC), Spain

Reviewed by:
Alejandra Navarro, Council for Agricultural and Economics Research (CREA), Italy
Dirk Vanderklein, Montclair State University, United States

***Correspondence:**
Da-Yong Fan
dayong.fan@anu.edu.au
Shou-Ren Zhang
zsr@ibcas.ac.cn

Specialty section:
This article was submitted to Plant Abiotic Stress, a section of the journal Frontiers in Plant Science

Received: *23 April 2020*
Accepted: *29 July 2020*
Published: *14 August 2020*

Citation:
Fan D-Y, Dang Q-L, Xu C-Y, Jiang C-D, Zhang W-F, Xu X-W, Yang X-F and Zhang S-R (2020) Stomatal Sensitivity to Vapor Pressure Deficit and the Loss of Hydraulic Conductivity Are Coordinated in Populus euphratica, a Desert Phreatophyte Species. Front. Plant Sci. 11:1248. doi: 10.3389/fpls.2020.01248

There are considerable variations in the percentage loss of hydraulic conductivity (*PLC*) at mid-day minimum water potential among and within species, but the underpinning mechanism(s) are poorly understood. This study tested the hypothesis that plants can regulate leaf specific hydraulic conductance (K_l) *via* precise control over *PLC* under variable $\Delta\Psi$ (water potential differential between soil and leaf) conditions to maintain the $-m/b$ constant ($-m$: the sensitivity of stomatal conductance to *VPD*; b: reference stomatal conductance at 1.0 kPa *VPD*), where *VPD* is vapor pressure deficit. We used *Populus euphratica*, a phreatophyte species distributed in the desert of Northwestern China, to test the hypothesis. Field measurements of *VPD*, stomatal conductance (g_s), g_s responses to *VPD*, mid-day minimum leaf water potential (Ψ_{lmin}), and branch hydraulic architecture were taken in late June at four sites along the downstream of Tarim River at the north edge of the Taklamakan desert. We have found that: 1) the $-m/b$ ratio was almost constant (=0.6) across all the sites; 2) the average Ψ_{50} (the xylem water potential with 50% loss of hydraulic conductivity) was –1.63 MPa, and mid-day *PLC* ranged from 62 to 83%; 3) there were tight correlations between Ψ_{50} and wood density/leaf specific hydraulic conductivity (k_l) and between specific hydraulic conductance sensitivity to water potential [$d(k_s)/d\ln(-\Psi)$] and specific hydraulic conductivity (k_s). A modified hydraulic model was applied to investigate the relationship between g_s and *VPD* under variable $\Delta\Psi$ and K_l conditions. It was concluded that *P. euphratica* was able to control *PLC* in order to maintain a relatively constant $-m/b$ under different site conditions. This study demonstrated that branchlet hydraulic architecture and stomatal response to *VPD* were well coordinated in order to maintain relatively water homeostasis of *P. euphratica* in the desert. Model simulations could explain the wide variations of *PLC* across and within woody species that are often observed in the field.

Keywords: hydraulic model, xylem cavitation, leaf specific hydraulic conductance, stomatal conductance, water homeostasis

INTRODUCTION

A global convergence has been demonstrated in the relationship between drought-induced embolism and daily minimum xylem water potential (Choat et al., 2012; Choat et al., 2018). The safety margin of the plant hydraulic system refers to the difference between the daily minimum xylem water potential and the xylem water potential at which 50% of the hydraulic conductance is lost due to the cavitation of xylem vessels. Plants are generally able to maintain the integrity of their hydraulic system within the safety margin by the stomatal regulation of water loss to maximize the carbon gain without the risk of catastrophic hydraulic failure. However, the functional association between minimum xylem water potential and hydraulic safety does not prove that all the plants can control embolisms to the same extent because *PLC* is a function of water potential, Ψ_{50}, and the slope of the cavitation vulnerability curve. As such, there are considerable inter- and intra-specific variations in *PLC* at the daily minimum xylem water potential (Pockman and Sperry, 2000; Johnson et al., 2009b; Fan et al., 2018). However, the underpinning mechanism(s) are not fully understood.

The stomatal regulation of xylem pressure is a function of vapor pressure deficit (*VPD*), leaf specific hydraulic conductance (K_l), soil water potential (Ψ_s), and leaf water potential (Ψ_l) (see **Table 1** for the definitions of major acronyms/symbols in the present study) according to the following simplified hydraulic model (Oren et al., 1999; Landsberg et al., 2017):

$$g_l = K_l \cdot (1/VPD) \cdot (\Psi_s - \Psi_l) \quad (1)$$

Where g_l is leaf conductance to water vapor, which is a function of boundary layer conductance to water vapor (g_{bl}) and stomatal conductance (g_s). It has been demonstrated that the sensitivity of stomatal conductance to *VPD* ($-m$) has a close relationship with the stomatal conductance at 1 kPa VPD (b) and the $-m/b$ ratio is found to be 0.6 for various mesic species across a variety of growth forms and habitats (Dang et al., 1997; Oren et al., 1999; Bucci et al., 2005; Landsberg et al., 2017) and the relationship is described as follows:

$$g_s = m \cdot \ln VPD + b \quad (2)$$

The above models predict that if K_l decreases due to xylem cavitation, the $-m/b$ ratio will need to increase because a more sensitive stomatal response is required to keep transpiration and $\Delta\Psi$ ($=\Psi_S - \Psi_l$, *i.e.*, water potential difference between soil and leaf) relatively constant (Oren et al., 1999; Landsberg et al., 2017). Furthermore, the large variations in *PLC* (which regulates K_l) will likely lead to variations in the $-m/b$ ratio. However, it is unlikely in nature that $\Delta\Psi$ remains constant when K_l varies even in isohydric species (Mcdowell, 2011). Therefore, the assumption of constant $\Delta\Psi$ needs to be relaxed. In this study, we simultaneously examined stomatal conductance to water vapor pressure deficit, the response of branch and leaf hydraulic conductance to water potential differential between leaf and soil, and xylem vulnerability to cavitation. We conducted the study on four populations of a desert phreatophyte tree species, *Populus euphratica*, along a gradient of water table depths. We test the hypothesis that if stomata are perfectly efficient in regulating leaf water status as indicated by a constant $-m/b$ both within and between species (Oren et al., 1999; Ewers et al., 2000), plants would fine-tune K_l *via* precise control over *PLC* (control the embolism degree) under variable $\Delta\Psi$ and K_l conditions. The results can provide an explanation for the considerable inter- and intra-specific variations in *PLC* at the daily minimum xylem water potential in the field.

From Equation 1, g_l can be obtained with the input of K_l, *VPD*, Ψ_l, and Ψ_s, while K_l is the product of maximum K_l and *PLC*. g_s can be obtained provided g_{bl} is known. Then $-m/b$ can be calculated based on Equation 2. Among all parameters required by the model, K_l, *VPD*, Ψ_l, and *PLC* can be measured/calculated in the field. In desert environment, g_{bl} is large and has minor impact on the model simulation (Comstock and Mencuccini, 1998; Oren et al., 1999). As such, the only obstacle to verify the above hypothesis for trees with a deep root system is that it is difficult to know the water availability in the entire rhizosphere because of the difficulty in obtaining a reliable Ψ_s, mainly due to the temporal–spatial soil moisture heterogeneity and nocturnal transpiration (Kavanagh et al., 2007; Landsberg et al., 2017). In this study, we used *Populus euphratica*, an obligate phreatophyte

TABLE 1 | List of symbols, abbreviations and their units.

Symbol/ Abbreviations	Definition	Units
a	vulnerability curve steepness	
b	reference conductance at *VPD* = 1 kPa	mmol m^{-2} s^{-1}
$d(k_s)/d\ln(-\Psi)$	sensitivity of k_s to decreasing water potential	kg m^{-1} MPa^{-2} s^{-1}
g_{bl}	the boundary layer conductance to water vapor	mmol m^{-2} s^{-1}
g_l	leaf conductance to water vapor	mmol m^{-2} s^{-1}
g_s	stomatal conductance	mmol m^{-2} s^{-1}
g_{sm}	the maximum physiological g_s	mmol m^{-2} s^{-1}
Huber value	the total cross-section sapwood area per unit leaf area	m^2 m^{-2}
k_l	leaf specific hydraulic conductivity,	kg m^{-1} MPa^{-1} s^{-1}
k_s	specific conductivity	kg m^{-1} MPa^{-1} s^{-1}
K_h	the maximum hydraulic conductivity	kg m MPa^{-1} s^{-1}
K_{hi}	the hydraulic conductivity measured at pressure i	kg m MPa^{-1} s^{-1}
K_l	leaf specific hydraulic conductance	mmol m^{-2} MPa^{-1} s^{-1}
$-m$	the sensitivity of g_s to *VPD*	mmol m^{-2} s^{-1} ln $(kPa)^{-1}$
$-m/b$	the sensitivity of g_s to *VPD* standardized by the stomatal conductance at 1.0 kPa *VPD*	
PLC	percentage loss of hydraulic conductivity	
T_r	transpiration rate	mol m^{-2} s^{-1}
VPD	leaf vapor pressure deficit	kPa
WD	woody density	g dry mass cm^{-3}
Ψ	the negative of the injection pressure for vulnerability curve establishment	MPa
Ψ_l	leaf water potential	MPa
Ψ_{min}	daily minimum branchlet xylem water potential	MPa
Ψ_{lmin}	daily minimum leaf xylem water potential	MPa
Ψ_s	soil water potential	MPa
$\Delta\Psi$	water potential differential between soil and leaf	MPa

species, to test the hypothesis. Because the root system of phreatophytes can reach and access the groundwater to avoid drought stress (Pockman and Sperry, 2000; Choat et al., 2012; Volaire, 2018), the $\Delta\Psi$ is largely determined by Ψ_l because Ψ_s is close to zero and the gravitational potential (−0.01MPa m^{-1}) is ignorable for groundwater tables of a few meters (Scholander et al., 1965). *P. euphratica* mainly grows along the riverside of Tarim River at the north edge of the Taklimakan Desert, NW China. Previous greenhouse studies have found that stems of *P. euphratica* seedlings are highly vulnerable to cavitation (high Ψ_{50}) and considerable *PLC* occurs at noon (Hukin et al., 2005), but there are no such field studies on this species. Thomas et al. (2008) and Gries et al. (2003) have found associations between g_s, *VPD*, k_l, and Ψ_l, but the relationship between stomatal sensitivity to *VPD* and hydraulic traits is still poorly understood. We hypothesize that the stomatal response to *VPD* and xylem response to water potential are functionally converged to maintain a functional coherence and integrity of the hydraulic system of the tree.

MATERIALS AND METHODS

Study Site

The study was carried out at four sites along the downstream of Tarim River (elevation of 931 m) in the Xinjiang Uighur Autonomous Region, NW China (**Figure 1**). The four sites are located at least 138 km east of Korla, at the northern fringe of the Taklamakan desert. Korla has a warm temperate continental arid climate; the average length of the frost-free season is 210 days. The annual average temperature is about 11°C, the average annual precipitation is less than 60 mm, and the annual maximum evaporation is about 2,800 mm. The average maximum temperature and average minimum relative humidity in June are 30.9°C and 9.9% respectively.

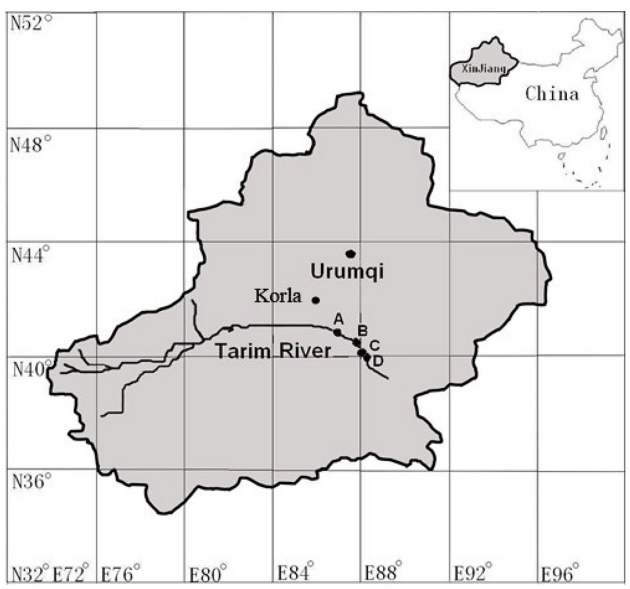

FIGURE 1 | Geological locations of the four studied sites. Site name: A = 31 Tuan, B = 33 Tuan, C = Yingsu, D = Alagan.

The four sites had natural *P. euphratica* stands with relatively uniformly distributed trees. The stand density was 100–300 stems per hectare. Four to five trees with diameter at breast height of 30–40 cm were selected from each site and south-facing sunlit branchlets, and leaves at 1.3–1.5 m height from the outermost part of the lower canopy were selected for measuring *in situ* g_s and hydraulic characteristics. Two branches per tree were selected for the branch architecture measurement and one to two leaves per tree were used to measure *in situ* g_s response to *VPD*. The groundwater tables of the four sites measured at local wells within 1 km from the sites were 2.49, 3.49, 4.46, and 7.92 m, respectively, for site 31 Tuan (site A), 33 Tuan (site B), Yingsu (site C) and Alagan (site D).

Measurements of g_s Response to *VPD*

g_s responses to *VPD* were measured on clear days in the field around noon (12:00 to 14:00 h) in late June under two sets of conditions: (1) controlled *VPD* and (2) un-controlled natural *VPD*, using a Li 6400 open gas exchange system (Li-Cor Cooperate, Lincoln, NE, USA). In the controlled-*VPD* measurements, a range of *VPD* from 0.8 to 3.5 kPa was achieved by using the apparatus on the equipment to vary the mixing ratio of water-vapor saturated air and dry air (after passing through desiccant). When the relative humidity in the leaf chamber exceeded 80% (*VPD* was about 0.8 kPa), the instrument displayed a warning sign of "High humidity alert", g_s and intercellular carbon dioxide concentration (C_i) readings fluctuated (*e.g.*, C_i fluctuated from negative to very large values), indicating the g_s measurement was not reliable. Therefore, data points with *VPD* values less than 1 kPa were discarded. Other environmental conditions in the leave cuvette were set as follows: Leaf temperature 31°C, Photosynthetically active radiation (PAR) 1,200 μmol m^{-2} s^{-1}, CO_2 concentration 390 μmol mol^{-1}. Only steady-state g_s readings at each *VPD* were recorded (Dang et al., 1997; Dang, 2013). Measurements under un-controlled natural *VPD* were taken in June and again in July. The conditions in the leaf chamber were set the same in in the two measurements (Leaf temperature 31°C, PAR 1,200 μmol m^{-2} s^{-1}, CO_2 concentration 390 μmol mol^{-1}). The $-m$ and b were estimated using Equation 2 and the non-linear regression model with gnls () function of the R software (R Development Core, 2017).

Leaf Water Potential and Branchlet Xylem Water Potential Measurements

The daily minimum leaf xylem water potential (Ψ_{lmin}) was measured in the field between 12:00 and 14:00 using a Scholander pressure chamber (PMS Instrument, Corvallis, Oregon, USA). The measurements were taken on the same trees on which the *VPD* responses were measured. The daily minimum branchlet xylem water potential (Ψ_{min}) was estimated according to the method of Pockman and Sperry (2000): a branchlet of similar size to that used in subsequent cavitation

vulnerability measurements was selected and sealed in a plastic bag containing a moist paper towel for 30 min in darkness to allow the equilibration of water potential between leaves and the subtending branchlet before a leaf was sampled and the petiole water potential was measured.

Cavitation Vulnerability Curve Measurement

A branchlet (50–70 cm long, 2–4 year-old) near that used for the g_s–*VPD* response measurement was cut from each sample tree before sunrise (before 8:00 AM) to measure k_l and the cavitation vulnerability curve. The branchlet was wrapped in moist paper towels immediately after being cut and transported to the laboratory. The maximum vessel length was measured from six samples randomly chosen from all the four sites together, based on the method (pressurized gas bubble under water) of Jacobsen et al. (2007). Since the maximum measured vessel length was less than 21 cm, all the samples (7–10 per site) were re-cut to 22–24 cm under water, and all the measurements were carried out in an air-conditioned laboratory (26°C). The maximum flow rate was measured under 8 kPa hydrostatic pressure after air emboli were flushed out by perfusion with 110 kPa distilled water (flowing through 0.2 μm filter) for 30 min. Measurements were initiated after ~2 min when the flow rate stabilized. The weight of the collected efflux was measured every 30 s with a precision balance (Sartorius, BP221S, Göttingen, Germany) to obtain the flow rate. Maximum k_l was calculated by dividing the maximum flow rate by the total leaf area distal to the measured segment and by the pressure gradient. The leaf area was determined using a WinFOLIA system (Regent Instruments, Quebec City, Canada). k_s was calculated by dividing the maximum flow rate by the segment's cross-section sapwood area. The total acropetal-end cross-section area of the branch segment was determined from its maximum and minimum diameter. The area of the pith was determined from its dimensions measured under a dissecting microscope equipped with a stage micrometer and subtracted from the above acropetal-end cross-section area to determine the cross-section sapwood area. The Huber value was calculated as the total cross-section sapwood area per unit leaf area (Tyree and Sperry, 1988).

The vulnerability of xylem to cavitation was characterized using a vulnerability curve which was measured using a Cavitation pressure chamber (PMS Instrument, Corvallis, Oregon, USA) according to Sperry and Saliendra (1994). A branch segment was inserted into a collar and sealed with both ends protruding. Air was injected into the collar at a set pressure, which was maintained for 15 min and then slowly decreased to 0.1 MPa. The hydraulic conductivity was then re-measured at a higher pressure. This procedure was repeated until at least 85% loss of hydraulic conductivity was reached. The *PLC* following each pressurization was calculated as $PLC = 100 \times (K_h - K_{hi})/K_h$, where K_{hi} is the hydraulic conductivity measured at pressure i. The vulnerability curve for each sample was fitted with an exponential sigmoidal equation (Pammenter and Vander Willigen, 1998):

$$PLC = \frac{100}{1 + e^{a(\Psi - \Psi_{50})}} \quad (3)$$

where Ψ is the negative of the injection air pressure and coefficients a and Ψ_{50} are estimated using a non-linear regression model with gnls() function of R software (R Development Core, 2017). Ψ_{50} represents the xylem water potential at which 50% of the hydraulic conductance is lost, a represents the steepness of vulnerability curve. k_l at noon was estimated from Ψ_{min}, the vulnerability curve, and maximum k_l (Pockman and Sperry, 2000; Johnson et al., 2009b).

Wood Density and k_s Sensitivity to Water Potential

Wood density (*WD*) was measured on stem segments used in the measurement of vulnerability curves after the removal of pith and bark, and the fresh volume was measured by the Archimedes principle of water displacement. The dry mass was determined after drying at 104°C for 24 h. *WD* is expressed as dry mass per unit fresh volume (g cm^{-3}).

Specific hydraulic conductance sensitivity to water potential [$d(k_s)/dln(-\Psi)$] was calculated based on the method by Ewers et al. (2000): we related maximum k_s, obtained at $-\Psi = 0$, to the branchlet k_s sensitivity to decreasing Ψ from −0.5 to −3.0 MPa. The slope of the $-\Psi$–k_s relationship was linearized by using the natural logarithm of $-\Psi$, and the logarithm transformation resulted in a good fit (R^2 = 0.91 to 0.95).

The Hydraulic Model

We used Equation 1 and the following equation:

$$g_l = (g_s \cdot g_{bl})/(g_s + g_{bl}) \quad (4)$$

to model the response of g_s to *VPD* at noon. We set constraints for g_{sm} (the maximum physiological g_s for *P. euphratica*), g_{bl}, K_l, and $\Delta\Psi$ according to the corresponding measured physiological range for *P. euphratica*. It is assumed that g_s had an upper limit of g_{sm} which was set as 1,000 mmol m^{-2} s^{-1}, based on our field measurements and the reported values for poplars (Hacke, 2015). The g_{bl} for desert environment was set as 2,000 mmol m^{-2} s^{-1} (Comstock and Mencuccini, 1998). K_l at noon was set between 0.5 and 4.0 mmol MPa^{-1} m^{-2} s^{-1}. $\Delta\Psi$ at noon ($\Psi_s - \Psi_{lmin}$) was set at 2.0 to 3.2 MPa according to the measured range of Ψ_{lmin} in the field. *VPD* was allowed to vary between 1 and 4 kPa, similar to the range observed in the field (Gries et al., 2003). Before running the simulation, we calculated K_l at noon from the estimated k_l at noon, assuming hydraulic path length = underground water table + sample height + branch length, and hydraulic conductance was uniformly distributed along the flow path from soil to branchlet (Pockman and Sperry, 2000). Note the unit of k_l is kg m^{-1} MPa^{-1} s^{-1}, and the unit of K_l is mmol m^{-2} MPa^{-1} s^{-1}. We converted the unit *VPD* into the unit of mol mol^{-1} as required by the model. We relaxed the assumption of constant $\Delta\Psi$ when exploring the relationship between K_l and $-m/b$. By allowing K_l and $\Delta\Psi$ to vary simultaneously, the g_s responses to *VPD* ($-m/b$) under all the combinations of K_l and $\Delta\Psi$ were solved. The simulation procedure was as follows (Oren et al., 1999): 1) the K_l and $\Delta\Psi$ were assigned to specific values; 2) g_l as the function of *VPD* was calculated from Equation 1; 3) g_s was solved from Equation 4; 4) when $g_s > g_{sm}$ (occurred

occasionally), we set $g_s = g_{sm}$ and re-solved the equation for $\Delta\Psi$; 5) the calculated g_s and assigned *VPD* were fitted by a non-linear regression model with the gnls () function of R software (R Development Core, 2017) to obtain $-m/b$ from Equation 2; 6) a semi-contour plot $-m/b$ *versus* $\Delta\Psi$ and K_l was constructed.

Statistical Analyses

The distribution normality of branchlet xylem hydraulic traits and leaf water status data were tested by calculating the Shapiro–Wilk W statistics for each sample (n = 4–5 for leaf water status variables, n = 7–10 for branchlet xylem hydraulic traits). Differences between sites were tested using Kruskl–Wallis H test if P(W) < 0.05. The Spearman rank correlation analysis was applied to investigate correlations among branchlet xylem hydraulic traits. ANOVA and Pearson correlation analysis were subsequently conducted if P(W) > 0.05. We conducted all the statistical analyses using R version 3.4.0 (R Development Core, 2017).

RESULTS

g_s, Ψ_{lmin}, b were significantly lower, and *VPD* was significant higher at Alagan than other sites (**Table 2**). Transpiration rate (T_r), $-m$, and $-m/b$ (0.57–0.61) were not significantly different among the four sites (**Table 2**). Differences in all the traits were smallest between 31 Tuan site and Yingsu site than among all the sites.

The branchlet hydraulic architecture of *P. euphratica* also varied with site (**Table 3**). Yingsu had significantly greater k_s, k_l, and $d(k_s)/dln(-\Psi)$ than the other three sites (**Table 3**). Huber value was lowest at Alagan and highest at 33 Tuan among the four sites although their differences from 31 Tuan and Yingsu were not statistically significant (**Table 3**). *WD* was lowest at 31 Tuan and highest at Alagan, but their differences from 33 Tuan and Yingsu were not statistically significant (**Table 3**). Ψ_{min} had the same trend as Ψ_{lmin}, *i.e.*, significantly more negative at Alagan than at all other sites, while there was no significant difference among the other sites (**Tables 2** and **3**). Ψ_{50} was most negative at Alagan (−2.22 MPa) and the least negative at Yingsu (−1.22 MPa) among the four sites, but the trend for a was the opposite (**Table 3**).

As there was no significant difference in $-m/b$ among the sites, we pooled all the *VPD* response data from the four sites and evaluated the general relationship between g_s and *VPD* for the species. We fit Equation 1 separately for the two sets of *VPD* response data. The estimated $-m/b$ was 0.607 for the controlled-*VPD* data set and 0.615 for the natural *VPD* field measurement (**Figures 2A, B**). $-m$ was positively correlated with b across the individuals of the four sites (**Figure 2C**).

The estimated *PLC* ranged from 62% at Alagan site to 83% at Yingsu site (**Figure 3**). The corresponding estimated k_l at noon for 31 Tuan, 33 Tuan, Yingsu, and Alagan sites was 1.11×10^{-4}, 1.09×10^{-4}, 1.12×10^{-4}, and 1.16×10^{-4} kg m^{-1} MPa^{-1} s^{-1}, respectively.

k_s was positively correlated with k_l (F = 6.637, P = 0.014), negatively correlated with Huber value (F = 19.407, P < 0.001) (**Table 4**). However, k_s showed no significant relationship with safety (Ψ_{50}) (F = 1.917, P = 0.175) (**Table 4**). There was a negative association between Ψ_{50} and *WD* (F = 8.566, P = 0.006) across the four sites (**Table 4**, **Figure 4A**). There was a positive correlation between Ψ_{50} and k_l (F = 5.937, P = 0.017) (**Table 4**, **Figure 4B**); k_l also showed a positive correlation with the reference stomatal conductance at 1.0 kPa (F = 37.274, P = 0.009) at the population scale (**Figure 4C**). $d(k_s)/dln(-\Psi)$ was positively correlated with k_s (F = 680.782, P < 0.001) (**Figure 4D**) across the individuals, and b at the population scale (F = 33.249, P = 0.01) (**Figure 4F**), but had no relationship with Ψ_{50} (F = 0.438, P = 0.51) (**Figure 4E**). There was no association between g_s and Ψ_{lmin} at the population scale (F = 12.047, P = 0.071) (**Figure 4H**). There was no significant

TABLE 2 | Means and standard error of the mean for g_s, T_r, *VPD*, Ψ_{lmin}, $-m$, b and $-m/b$ at the four sites.

Population	g_s	T_r	*VPD*	Ψ_{lmin}	$-m$	b	$-m/b$
31 Tuan	536 ± 68^{a}	7.28 ± 1.48^{a}	1.56 ± 0.10^{b}	−2.30 ± 0.03^{a}	518.9 ± 130.6^{a}	802.5 ± 102.9^{a}	0.61 ± 0.10^{a}
33 Tuan	396 ± 39^{ab}	7.62 ± 0.63^{a}	1.96 ± 0.10^{b}	−2.55 ± 0.05^{a}	333.7 ± 54.8^{a}	588.1 ± 72.0^{ab}	0.57 ± 0.07^{a}
Yingsu	490 ± 41^{a}	8.73 ± 0.90^{a}	1.88 ± 0.22^{b}	−2.45 ± 0.06^{a}	435.2 ± 60.0^{a}	769.7 ± 8.3^{a}	0.57 ± 0.08^{a}
Alagan	328 ± 39^{b}	8.07 ± 0.65^{a}	2.46 ± 0.08^{a}	−3.01 ± 0.09^{b}	328.3 ± 33.2^{a}	577.1 ± 35.7^{b}	0.58 ± 0.08^{a}
P value	≤0.05	>0.05	≤0.05	≤0.05	>0.05	>0.05	>0.05

Symbols, their definition and units are provided in ***Table 1****.*
Different letters among populations indicate significant difference at p = 0.05.

TABLE 3 | Means and the standard error of the mean for k_s, k_l, *WD*, Ψ_{min}, Huber value, Ψ_{50}, $d(k_s)/dln(-\Psi)$, and a at the four sites.

Population	k_s	k_l(×10^{-4})	*WD*	Ψ_{min}	*Huber*(×10^{-4})	Ψ_{50}	a	$d(k_s)/dln(-\Psi)$
31 Tuan	1.52 ± 0.16^{b}	3.51 ± 0.43^{b}	0.405 ± 0.035^{b}	−2.14 ± 0.06^{a}	2.79 ± 0.34^{ab}	−1.39 ± 0.12^{ab}	1.71 ± 0.16^{a}	0.59 ± 0.06^{b}
33 Tuan	1.51 ± 0.34^{b}	3.68 ± 0.28^{b}	0.491 ± 0.007^{ab}	−2.27 ± 0.16^{a}	3.05 ± 0.35^{a}	−1.67 ± 0.15^{b}	1.35 ± 0.15^{ab}	0.49 ± 0.15^{b}
Yingsu	2.94 ± 0.36^{a}	6.63 ± 0.84^{a}	0.474 ± 0.006^{ab}	−2.23 ± 0.08^{a}	2.40 ± 0.36^{ab}	−1.22 ± 0.23^{a}	1.72 ± 0.19^{a}	1.08 ± 0.20^{a}
Alagan	2.02 ± 0.49^{b}	3.04 ± 0.35^{b}	0.496 ± 0.010^{a}	−2.73 ± 0.03^{b}	31.63 ± 0.22^{b}	−2.22 ± 0.11^{c}	0.94 ± 0.08^{b}	0.83 ± 0.17^{ab}
P value	≤0.01	≤0.001	≤0.01	≤0.001	≤0.01	≤0.001	≤0.01	≤0.05

Symbols, their definition, and units are given in ***Table 1****.*
Different letters among populations indicate significant difference at p = 0.05.

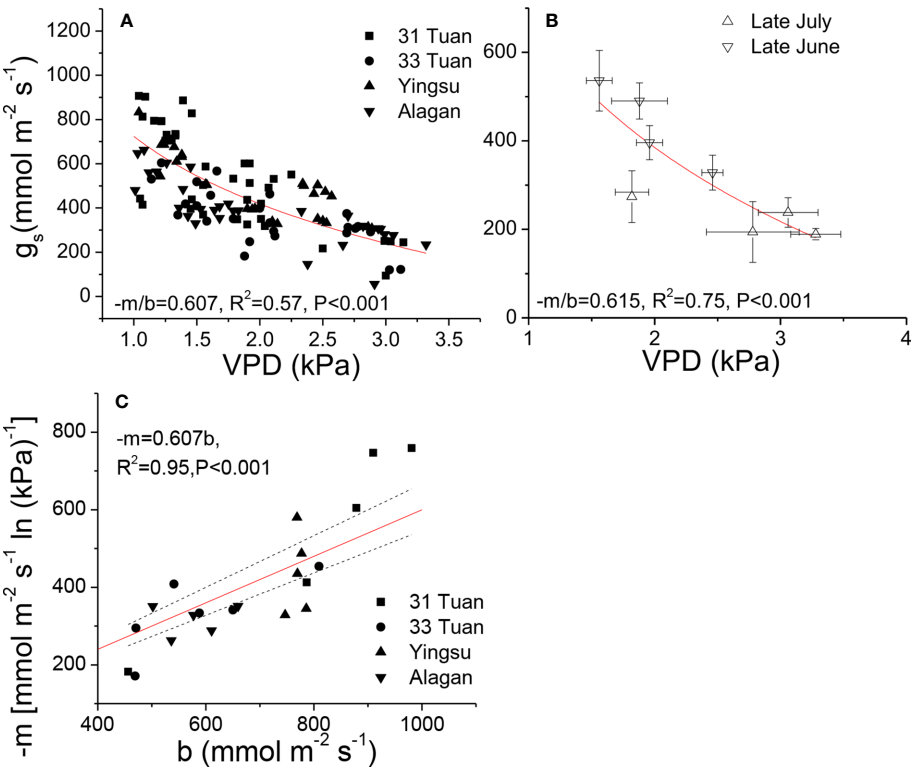

FIGURE 2 | Relationships between g_s and *VPD* **(A, B)**, and the relationship between $-m$ and b **(C)** of *Populus euphratica* among the four sites. The measurements were taken by manipulating *VPD* in late June **(A, C)**, and natural *VPD* in late June and late July **(B)**. The curves were generated by using the hydraulic model (Equation 1). In **(C)**, red line represents the theoretical line of the expected relationship ($-m = 0.6b$), black dash lines represent 95% confidence intervals of linear regression between observed $-m$ and b.

relationship between g_s and T_r (F = 0.99, P = 0.33) (**Figure 4G**). There was also a marginally positive association (F = 13.048, P = 0.061) between Ψ_{50} and Ψ_{min} across the four sites, and the slope of this relationship is similar to the slope for other angiosperm species in the world (**Figure 5**). The safety margin ($\Psi_{min} - \Psi_{50}$) was negative (*i.e.*, below the 1:1 line in **Figure 5**) because the actual measured Ψ_{min} was more negative than Ψ_{50} and the actual PLC was greater than 50%. g_s increased with increasing (*i.e.*, becoming less negative) Ψ_{min}, and the rate of increase was greater at sites with less negative Ψ_{min} (**Figure 4H**).

Figure 6 demonstrated the effect of $-m/b$ on the relationship between K_l and $\Delta\Psi$. The average values of K_l and $\Delta\Psi$ around noon for the four sites all fell well within the range of 0.58–0.60 $-m/b$. Belt A and belt B in **Figure 6** were within the same $-m/b$ range (0.58–0.60) but different K_l at noon. Belt C had a $-m/b$ range of 0.62–0.64, but its K_l at noon was higher than belt A but lower than belt B.

DISCUSSION

The Ψ_{50} values measured in this study are within the range of values reported for poplar trees around the world, *e.g.*, −1.30 MPa for *P. tremula*, −2.95 MPa for *P. nigra* (Choat et al., 2012), −0.69 MPa for *P. deltoids*, and −2.75 MPa for *P. tremuloides* (Fichot et al., 2015). Hukin et al. (2005) have reported that *P. euphratica* seedlings have a Ψ_{50} for xylem cavitation of only −0.7 MPa, while the field-grown *P. euphratica* trees in our study had an average Ψ_{50} of −1.63 MPa across the four sites. These results suggest that the seedlings of *P. euphratica* may be much more vulnerable to xylem cavitation than trees at a later developmental stage. Although the seedlings of *P. euphratica* were measured at a different location in a different study (Hukin et al., 2005) from the larger trees, the response trend is consistent with that of another poplar species, *P. tremuloides*, the field grown trees which have a Ψ_{50} of −2.75 MPa (Sperry and Sullivan, 1992) while its seedlings only −0.68 to −0.84 MPa (Way et al., 2013). Furthermore, the value of Ψ_{50} that we measured on *P. euphratica* in this study (−1.63 MPa) is much less negative than the reported values for other drought resistant tree species, *e.g.*, −2.75 MPa for *P. tremuloides* (Sperry and Sullivan, 1992), −8.42 MPa for *Pistacia terebinthus* (Maherali et al., 2004), suggesting that *P. euphratica* may be more vulnerable to cavitation than other drought tolerant desert species. Our measurement of *PLC* was in line with the mid-day *PLC* of 76% reported by Zhou et al. (2013).

The results of this study suggest that *P. euphratica* is a mesic-adapted species. In a mesic-adapted species, g_s generally has a much tighter relationship with *VPD* (**Figures 2A, C**) than with k_s

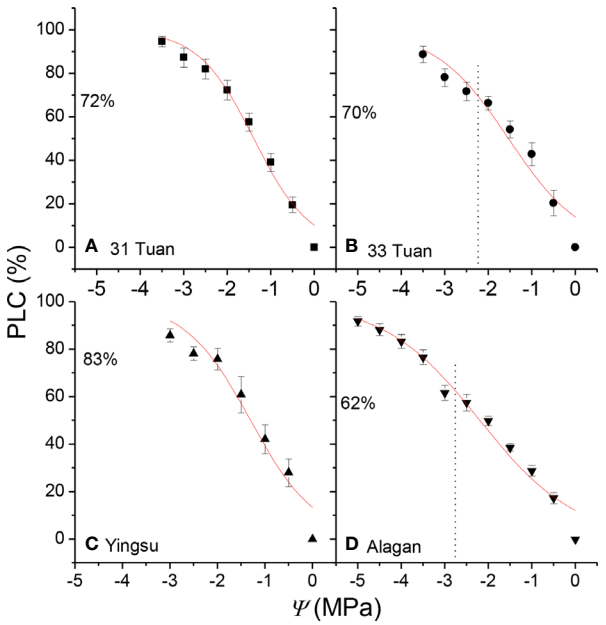

FIGURE 3 | *PLC* as a function of Ψ for the four populations of *Populus euphratica* (means ± 1 se). The curves were fitted using all data points. The vertical dotted line indicates the position of measured Ψ_{min}; the horizontal dotted line indicates the percentage loss of hydraulic conductivity at Ψ_{min}. The number under the horizontal dotted line is the *PLC* at noon. See **Table 1** for the definition of symbols.

TABLE 4 | Pearson correlations between branchlet hydraulic traits of *Populus euphratica*.

	k_s	k_l	*WD*	*Huber*	Ψ_{50}
k_s	1				
k_l	0.399**	1			
WD	0.236^{ns}	0.06 ^{ns}	1		
Huber	$^{-}$0.581***	0.265 ^{ns}	$^{-}$0.172 ^{ns}	1	
Ψ_{50}	$^{-}$0.228 ^{ns}	0.355*	$^{-}$0.443**	0.387**	1

Symbols, their definition, and units can be found in ***Table 1****.*
, **, * and ns denote significance at P ≤ 0.05, P ≤ 0.01, P ≤ 0.001 and no significant difference, respectively.*

(F = 0.02, P = 0.89 at the population scale) or T_r (**Figure 4G**) (Thomas et al., 2008; Yu et al., 2019), and $-m$ is generally converged at 0.6 when standardized by b (Oren et al., 1999). The $-m/b$ value of 0.6 is consistent with the prediction of the hydraulic model (Equation 1) that assumes that stomatal conductance controls the leaf water potential and transpiration rate under full irradiance. Both our controlled-*VPD* experiment and the measurements of g_s response to natural *VPD* measured under field conditions across all four sites confirmed that the $-m/b$ value was approximately 0.6 for *P. euphratica*. The results also support the hypothesis that the hydraulic homeostasis of phreatophyte species is restricted by transpiration water demand (*VPD*) but not by the water supply in the soil because their root system can uptake water directly from the groundwater, and thus their water supply remains largely stable throughout the year (Thomas et al., 2000; Bruelheide et al., 2003). The nearly isohydric behavior could also be demonstrated by the close association between $-m$ and b across the individuals from the four populations (**Figure 2C**). The high xylem vulnerability and the pattern of g_s response to *VPD* found this study provide physiological explanations for some of the ecological phenomena that are often observed in the field, *e.g.*, very little sexual reproduction (Hukin et al., 2005), extensive clonal growth (Bruelheide and Jandt, 2004). We observed that there were very few seedlings at the four sites of this study. The limited number of seedlings on the sites may have been a result of the inability of seedlings to access the ground water, particularly during the dry season. The groundwater table generally deepens as a result of the management of the river system (Chen et al., 2015). In order to survive a drought spell, the root system of the seedlings must be able to reach and access the groundwater because of the high vulnerability to xylem cavitation and the inability of the species to effectively control water loss when the transpirational demand is high (*i.e.*, mesic g_s response to *VPD*). Because the root system of seedlings generally cannot penetrate deep enough to tap the groundwater as the ground table deepens or if they grow far away from the river bank, the mortality rate of tree seedlings is very high (Chen et al., 2015), leading to a lower rate of successful sexual regeneration. Consequently, the proportion of vegetative regeneration from suckering generally increases with increasing distance from the river bank. Similar phenomena on *P. euphratica* have been reported by other studies (*e.g.*, Wu et al., 2010). These results suggest that the distribution of this species in the desert primarily depends on its access to groundwater (Gries et al., 2003).

The "safety margin" ($\Psi_{min} - \Psi_{50}$) of *P. euphratica* ranged from −0.5 to −1.01 MPa across the four sites in this study. While these values are within the general range of values reported for other tree species in the world that grow under comparable environmental conditions to those of our study sites (Choat et al., 2012), *P. euphratica* tended to have a more negative Ψ_{min} than other species with the same Ψ_{50} (**Figure 5**). The linear regression line between Ψ_{min} and Ψ_{50} (marginally significant) had a similar slope to that of angiosperm species in the literature (Choat et al., 2012). suggesting that the species tended to regulate stomatal aperture to maintain water homeostasis but was less able to do so. However, the negative value of the safety margin suggests that *P. euphratica* operated beyond the hydraulic safety margin and thus suffered more than 50% loss of hydraulic conductivity around noon. Indeed, the *PLC* at noon ranged from 62% at Alagan to 83% at Yingsu site. Since it is generally believed that plants can fine-tune *PLC* to avoid catastrophic hydraulic dysfunction (Tyree and Sperry, 1988; Macinnis-Ng et al., 2004), it is puzzling why such large differences in *PLC* occurred in *P. euphratica* at different sites. We thus proposed that plants can fine-tune K_l *via* precise control over *PLC* to maintain a constant $-m/b$, according to the prediction of Equation 1 and Equation 2 (Oren et al., 1999; Ewers et al., 2000), which can provide insight into the mechanism underpinning the large variation of *PLC* in *P. euphratica*. The results further suggest that *P. euphratica* had a greater ability to restore cavitated xylem vessels daily than most

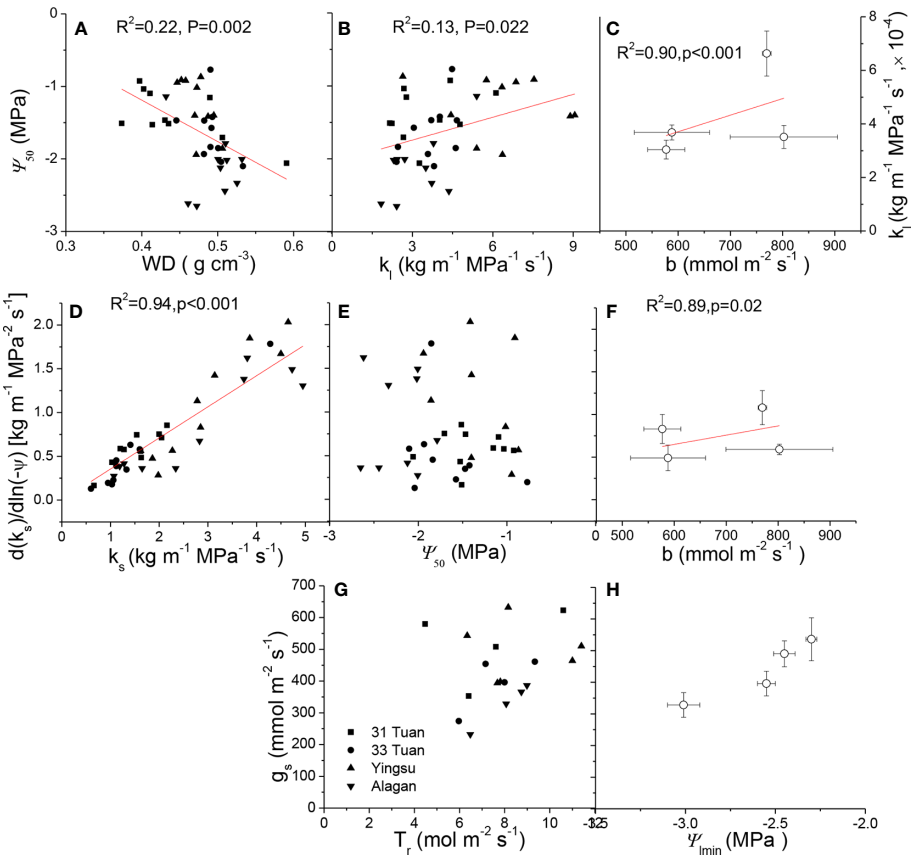

FIGURE 4 | Ψ_{50} as a function of: **(A)** *WD* and **(B)** k_l. k_l as a function of *b* at the population scale **(C)**. d(k_s)/dln(−Ψ) as a function of: **(D)** k_s, **(E)** Ψ_{50}, and **(F)** *b* at the population scale of *Populus euphratica* at the four sites. g_s as a function of: **(G)** T_r, and **(H)** Ψ_{min} at the population scale of *Populus euphratica* at the four sites. In **Figures 4C, F** and **H** , data were shown as mean ± 1 se. For relationships at the population scale, the four points are the means of the four sites.

angiosperm species. However, the factor or factors responsible for such a high ability are not clear and warrant investigations.

The results of this study suggest that the hydraulic model (Equation 1) and/or its assumptions may need to be modified when used to examine the relationship between K_l and $-m/b$. The model predicts that if K_l decreases due to xylem cavitation, the $-m/b$ will increase because a greater stomatal response is required to keep transpiration and $\Delta\Psi$ (Soil water potential minus leaf water potential) constant (Oren et al., 1999; Landsberg et al., 2017). However, the $-m/b$ in the current study was relatively constant (close to 0.6) across the four sites despite the large declines in K_l at noon. Furthermore, the model assumes that $\Delta\Psi$ remains constant when K_l varies, which unlikely occurs in nature. In this study, we allowed K_l and $\Delta\Psi$ to vary concurrently to relax the assumptions and set values for K_l, $\Delta\Psi$, g_{sm}, and g_{bl} based on the measured physiological ranges for *P. euphratica* in our investigation of the relationship between K_l and $-m/b$.

The output of the hydraulic model with our modifications was supported by our field measurements. The modeled relationship between K_l and $\Delta\Psi$ at noon for our four sites was within the band of 0.58–0.60 $-m/b$ (**Figure 6**), and the $-m/b$ range calculated from our field measurements was 0.57–0.61. The *in situ* native midday *PLC* for *P. euphratica* (76%) measured by Zhou et al. (2013) along the Arim River is also consistent with our modeled value. A 1:1 correspondence between native embolism and the embolism predicted from vulnerability curves for desert plants is also reported by Pockman and Sperry (2000). These results suggest that correctly constructed VC curves (Wheeler et al., 2013) and hydraulic models can reliably predict native embolism in the field. It is also reported that xylem embolism is likely a critical element for the decrease of leaf hydraulic conductance during the daytime (Kikuta et al., 1997; Woodruff et al., 2007; Johnson et al., 2009a; Zhang et al., 2016), particularly for poplar species (Laur and Hacke, 2014; Scoffoni et al., 2017). *P. euphratica* could tolerate more than 50% xylem cavitation around noon and that it regulated *PLC*s based on the different conditions of the four sites in order to achieve a similar stomatal sensitivity under the condition where water supply and irradiance were not limited. This hydraulic strategy might be critical for *P. euphratica* to maximize its carbon gain and facilitate its growth in an arid environment. It can be inferred that *P. euphratica* trees may have the capacity of

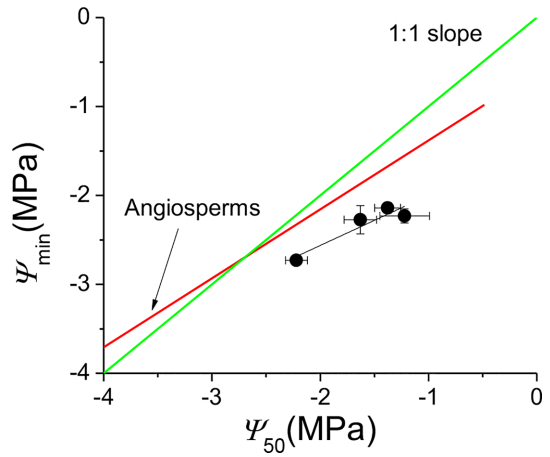

FIGURE 5 | Ψ_{min} as a function of Ψ_{50} for *Populus euphratica* at the four sites. The four black points are the means of the four sites. The red line is the regression line fitted using measurements for angiosperm species in the world (Choat et al., 2012). The F value and probability for the regression black line of *Populus euphratica* at the four sites are 14.76 and 0.061, respectively. The green line is the 1:1 regression line between Ψ_{min} and Ψ_{50}. Errors bars represent ± se.

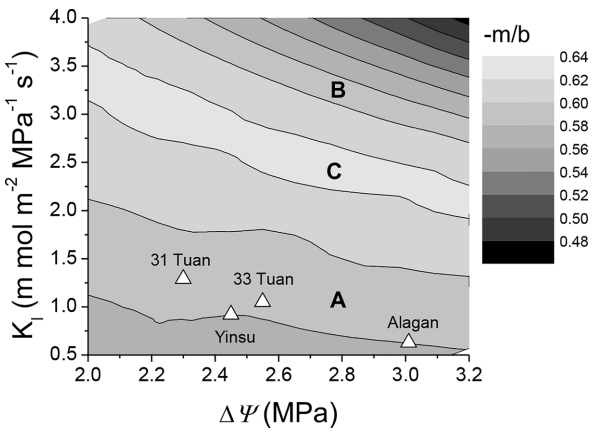

FIGURE 6 | Semi-contour plots of $-m/b$ as dependent on $\Delta\Psi$ and K_l. Plots are derived from the hydraulic model (Equation 1). The simulated $-m/b$ at the four studied sites are shown as (Δ). *A* and *B* in the figure represent belts with same $-m/b$ but different K_l at noon, *C* represents belt with higher $-m/b$ than *A* and *B*, but its K_l at noon is between those of *A* and *B*. Note the unit of K_l is mmol m^{-2} MPa^{-1} s^{-1}.

refilling the embolized xylem vessels or producing new vessels to restore the hydraulic capacity quickly (Gleason et al., 2016; Choat et al., 2018). However, the literature indicates that not all the species have the capacity to refill caviated vessels (Charrier et al., 2016; Torres-Ruiz, 2020). Further research in this area is warranted.

There are generally considerable variations in *PLC* at mid-day minimum xylem water potential among and within species (Pockman and Sperry, 2000; Johnson et al., 2009b; Fan et al., 2018), and based on the *PLC* at the mid-day water potential, a species can be classified into one of the two strategic groups: the conservative group (*PLC* < 50%) or the radical group (50% <*PLC* < 100%). Interestingly, the results of model simulation in the present study indicate that the two strategy groups could have similar stomatal sensitivity (*e.g.*, belt A for the radical strategy and belt B for the conservative strategy in **Figure 6** had the same range of stomatal sensitivity), suggesting that maintaining the theoretical threshold stomatal sensitivity ($-m/b$ = 0.6) is probably critical for the fitness of mesic species regardless of which strategy they adopt. A $-m/b$ above 0.62 (Belt C in **Figure 6**, with smaller *PLC* than the radical strategy and greater *PLC* than the conservative strategy) might be detrimental to photosynthesis because a small increase in *VPD* would induce a large decline in stomatal conductance and thus CO_2 supply for photosynthesis even when water supply and irradiance are not limited, possibly reducing the competitiveness of the species. However, the reason why *P. euphratica* has adopted the radical strategy (belt A in **Figure 6**) instead of the conservative strategy (belt B in **Figure 6**) remains unknown. It is possible that xylem cavitation may help plants to survive drought stress by rationing water use (Sperry, 1995) and temporally releasing the effects of water stress for a portion of the tree (Hölttä et al., 2011). It is also worth noting that *P. fremontii* (a riparian species in Sonoran desert), a comparable species to *P. euphratica*, has 16.5–31.97% embolism at noon (Pockman and Sperry, 2000) and is likely located in belt B of **Figure 6** and has adopted a conservative strategy.

The result that increased cavitation resistance was linked to increased wood density (**Figure 4A**) is expected because denser wood tends to be better able to sustain the compressive forces generated by lower negative pressures and to minimize air permeability that might cause xylem cavitation (Pockman and Sperry, 2000; Hacke et al., 2001; Bucci et al., 2013). Further, the positive relationship between k_l and Ψ_{50} (**Figure 4B**) suggests there was a functional trade-off between efficiency and safety at the leaf level. The positive relationship between k_s and $d(k_s)/dln(-\Psi)$ (**Figure 4E**) is coherent with the positive relationships between stomatal sensitivity to *VPD* and stomatal conductance at low *VPD* (*i.e.*, 1.0 kPa) and between leaf hydraulic conductance and stomatal conductance at low *VPD*, providing evidence to support the functional convergence between xylem and leaves. Furthermore, faster growing species or populations tend to have lower wood density, higher stomatal and xylem conductance but lower drought resistance. The curvilinear relationship between g_s and Ψ_{min} suggests that trees with less negative Ψ_{min} had higher but more sensitive g_s, which also coincided with lower wood density and higher hydraulic conductance as well as sites with shallower water tables. The results of this study provide physiological evidence for the mechanisms governing the tradeoff between growth rate, anatomy, physiological functioning, and stress resistance.

Transpiration is controlled by both vapor pressure deficit and leaf conductance. Therefore, it is not surprising that g_s was not significantly correlated to T_r (**Figure 4G**). The leaf conductance in turn is controlled by *VPD* and the internal water status as

demonstrated by Equations 1 and 2. Equation 1 demonstrates that leaf conductance is the linkage between the internal water relations in the tree and the moisture conditions of the ambient air. This conclusion can further enforced the coherent functional relationships discussed in the previous paragraph, such as the significant, linear relationship between $d(k_s)/d\ln(-\Psi)$ and k_s (**Figure 4D**). This relationship could facilitate the fine-tuning of *PLC* to sustain transpiration (Ewers et al., 2000) across the individuals (**Table 2**, **Figure 2**). More importantly, the lack of significant relationship between g_s and Tr/Ψ_{lmin} (**Figures 4G, H**) indicates that the hydraulic behavior of *P. euphratica* resembled that of an isohydric species, which is in consistence with the observation on *P. euramericana* (Tardieu and Simonneau, 1998) and several poplar genotypes (Navarro et al., 2018). The nearly isohydric behavior also indicates higher b (same meaning as $-m$, Oren et al., 1999) is functionally associated with higher $d(k_s)/d\ln(-\Psi)$ and higher k_l (at the population scale) (**Figures 4C, F**), consistent with the observation that stomata respond to changes in branchlet hydraulic conductance in a manner of feedback response to leaf water status (Saliendra et al., 1995). The results can be explained solely by hydraulic signaling or by an interaction between hydraulic and chemical signaling in the control of stomatal conductance (Tardieu and Simonneau, 1998; Comstock, 2002; Buckley, 2019; Qu et al., 2019).

In summary, this study demonstrates that the hydraulic architecture of branchlets and stomatal response to *VPD* were well coordinated with each other so that the water homeostasis of *P. euphratica* was maintained in the desert environment. The high xylem vulnerability to cavitation and the pattern of g_s response to *VPD* measured in the field further corroborated previous conclusions that the distribution and growth of *P. euphratica* in the desert solely depend on its access to groundwater (Gries et al., 2003; Hukin et al., 2005; Thomas et al., 2008). Thus, the populations of this phreatophyte species may decline if and when the groundwater table deepens as a result of reduced precipitation induced by global climate change, river management, or dam constructions (Zhou, 1993; Gries et al., 2003; Chen et al., 2015). We also demonstrated that the observed $-m/b$ of *P. euphratica* is consistent with the theoretical value derived from a simple hydraulic model when the assumption of constant $\Delta\Psi$ was relaxed. Our results demonstrate that model simulations can potentially explain the wide range of variations in *PLC* across and within woody species that is often observed in the field but further research efforts in this area is warranted.

DATA AVAILABILITY STATEMENT

The raw data supporting the conclusions of this article will be made available by the authors, without undue reservation.

AUTHOR CONTRIBUTIONS

D-YF and S-RZ designed the experiment. D-YF, C-DJ, X-WX, and X-FY carried out the experiment. D-YF, S-RZ, C-YX, and Q-LD performed the statistical analyses and drafted the manuscript. W-FZ assisted in the experiment. All authors commented on the manuscript. All authors contributed to the article and approved the submitted version.

FUNDING

This study was financially supported by the National Key Research and Development Program of China (2016YFA0 600802), State Key Project of Research and Development Plan (2016YFC0502104) and the Science and Technology Project of Beijing (Z171100004417019).

ACKNOWLEDGMENTS

We thank Dr. Ram Oren and two reviewers for their constructive comments and suggestions on the previous version of this manuscript, which have contributed substantially toward enhancing the quality of the manuscript.

REFERENCES

Bruelheide, H., and Jandt, U. (2004). "Vegetation types in the foreland of the Qira Oasis: present distribution and changes during the last decades," in *Ecophysiology and Habitat Requirements of Perennial Species in the Taklimakan Desert*. Eds. M. Runge and X. Zhang (Aachen, Germany: Shaker), 27–34.

Bruelheide, H., Jandt, U., Gries, D., Thomas, F. M., Foetzki, A., Buerkert, A., et al. (2003). Vegetation changes in a river oasis on the southern rim of the Taklamakan Desert in China between 1956 and 2000. *Phytocoenologia* 33, 801–818. doi: 10.1127/0340-269X/2003/0033-0801

Bucci, S. J., Goldstein, G., Meinzer, F. C., Franco, A. C., Campanello, P., and Scholz, F. G. (2005). Mechanisms contributing to seasonal homeostasis of minimum leaf water potential and predawn disequilibrium between soil and plant water potential in Neotropical savanna trees. *Trees* 19, 296–304. doi: 10.1007/s00468-004-0391-2

Bucci, S. J., Scholz, F. G., Peschiutta, M. L., Arias, N. S., Meinzer, F. C., and Goldstein, G. (2013). The stem xylem of P atagonian shrubs operates far from the point of catastrophic dysfunction and is additionally protected from drought-induced embolism by leaves and roots. *Plant Cell Environ.* 36, 2163–2174. doi: 10.1111/pce.12126

Buckley, T. N. (2019). How do stomata respond to water status? *New Phytol.* 224, 21–36. doi: 10.1111/nph.15899

Charrier, G., Torres-Ruiz, J. M., Badel, E., Burlett, R., Choat, B., Cochard, H., et al. (2016). Evidence for hydraulic vulnerability segmentation and lack of xylem refilling under tension. *Plant Physiol.* 172, 1657–1668. doi: 10.1104/pp.16.01079

Chen, Y., Li, W., Xu, C., Ye, Z., and Chen, Y. (2015). Desert riparian vegetation and groundwater in the lower reaches of the Tarim River basin. *Environ. Earth Sci.* 73, 547–558. doi: 10.1007/s12665-013-3002-y

Choat, B., Jansen, S., Brodribb, T. J., Cochard, H., Delzon, S., Bhaskar, R., et al. (2012). Global convergence in the vulnerability of forests to drought. *Nature* 491, 752–755. doi: 10.1038/nature11688

Choat, B., Brodribb, T. J., Brodersen, C. R., Duursma, R. A., Lopez, R., and Medlyn, B. E. (2018). Triggers of tree mortality under drought. *Nature* 558, 531–539. doi: 10.1038/s41586-018-0240-x

Comstock, J., and Mencuccini, M. (1998). Control of stomatal conductance by leaf water potential in Hymenoclea salsola (T. & G.), a desert subshrub. *Plant Cell Environ.* 21, 1029–1038. doi: 10.1046/j.1365-3040.1998.00353.x

Comstock, J. (2002). Hydraulic and chemical signalling in the control of stomatal conductance and transpiration. *J. Exp. Bot.* 53, 195–200. doi: 10.1093/jexbot/53.367.195

Dang, Q. L., Margolis, H. A., Coyea, M. R., Sy, M., and Collatz, G. J. (1997). Regulation of branch-level gas exchange of boreal trees: roles of shoot water potential and vapor pressure difference. *Tree Physiol.* 17, 521–535. doi: 10.1093/treephys/17.8-9.521

Dang, Q. (2013). Improving the quality and reliability of gas exchange measurements. *J. Plant Physiol. Pathol.* 1, 2. doi: 10.4172/jppp.1000e101

Ewers, B., Oren, R., and Sperry, J. (2000). Influence of nutrient versus water supply on hydraulic architecture and water balance in Pinus taeda. *Plant Cell Environ.* 23, 1055–1066. doi: 10.1046/j.1365-3040.2000.00625.x

Fan, D. Y., Zhang, S. R., Yan, H., Wu, Q., Xu, X. W., and Wang, X. P. (2018). Do karst woody plants control xylem tension to avoid substantial xylem cavitation in the wet season? *For. Ecosyst* 5, 40–50. doi: 10.1186/s40663-018-0158-7

Fichot, R., Brignolas, F., Cochard, H., and Ceulemans, R. (2015). Vulnerability to drought-induced cavitation in poplars: synthesis and future opportunities. *Plant Cell Environ.* 38, 1233–1251. doi: 10.1111/pce.12491

Gleason, S. M., Westoby, M., Jansen, S., Choat, B., Hacke, U. G., Pratt, R. B., et al. (2016). Weak tradeoff between xylem safety and xylem-specific hydraulic efficiency across the world's woody plant species. *New Phytol.* 209, 123–136. doi: 10.1111/nph.13646

Gries, D., Zeng, F., Foetzki, A., Arndt, S. K., Bruelheide, H., Thomas, F. M., et al. (2003). Growth and water relations of Tamarix ramosissima and Populus euphratica on Taklamakan desert dunes in relation to depth to a permanent water table. *Plant Cell Environ.* 26, 725–736. doi: 10.1046/j.1365-3040.2003.01009.x

Hacke, U. G., Sperry, J. S., Pockman, W. T., Davis, S. D., and Mcculloh, K. A. (2001). Trends in wood density and structure are linked to prevention of xylem implosion by negative pressure. *Oecologia*. 126, 457–461. doi: 10.1007/s004420100628

Hacke, U. G. (2015). "The hydraulic architecture of Populus," in *Functional and ecological xylem anatomy* (Cham: Springer), 103–131.

Hölttä, T., Juurola, E., Lindfors, L., and Porcar-Castell, A. (2011). Cavitation induced by a surfactant leads to a transient release of water stress and subsequent 'run away'embolism in Scots pine (Pinus sylvestris) seedlings. *J. Exp. Bot.* 63, 1057–1067. doi: 10.1093/jxb/err349

Hukin, D., Cochard, H., Dreyer, E., Le Thiec, D., and Bogeat-Triboulot, M. B. (2005). Cavitation vulnerability in roots and shoots: does Populus euphratica Oliv., a poplar from arid areas of Central Asia, differ from other poplar species? *J. Exp. Bot.* 56, 2003–2010. doi: 10.1093/jxb/eri198

Jacobsen, A. L., Pratt, R. B., Davis, S. D., and Ewers, F. W. (2007). Cavitation resistance and seasonal hydraulics differ among three arid Californian plant communities. *Plant Cell Environ.* 30, 1599–1609. doi: 10.1111/j.1365-3040.2007.01729.x

Johnson, D. M., Meinzer, F. C., Woodruff, D. R., and Mcculloh, K. A. (2009a). Leaf xylem embolism, detected acoustically and by cryo-SEM, corresponds to decreases in leaf hydraulic conductance in four evergreen species. *Plant Cell Environ.* 32, 828–836. doi: 10.1111/j.1365-3040.2009.01961.x

Johnson, D. M., Woodruff, D. R., Mcculloh, K. A., and Meinzer, F. C. (2009b). Leaf hydraulic conductance, measured in situ, declines and recovers daily: leaf hydraulics, water potential and stomatal conductance in four temperate and three tropical tree species. *Tree Physiol.* 29, 879–887. doi: 10.1093/treephys/tpp031

Kavanagh, K. L., Pangle, R., and Schotzko, A. D. (2007). Nocturnal transpiration causing disequilibrium between soil and stem predawn water potential in mixed conifer forests of Idaho. *Tree Physiol.* 27, 621–629. doi: 10.1093/treephys/27.4.621

Kikuta, S., Lo Gullo, M., Nardini, A., Richter, H., and Salleo, S. (1997). Ultrasound acoustic emissions from dehydrating leaves of deciduous and evergreen trees. *Plant Cell Environ.* 20, 1381–1390. doi: 10.1046/j.1365-3040.1997.d01-34.x

Landsberg, J., Waring, R., and Ryan, M. (2017). Water relations in tree physiology: where to from here? *Tree Physiol.* 37, 18–32. doi: 10.1093/treephys/tpw102

Laur, J., and Hacke, U. G. (2014). The role of water channel proteins in facilitating recovery of leaf hydraulic conductance from water stress in Populus trichocarpa. *PloS One* 9, e111751. doi: 10.1371/journal.pone.0111751

Macinnis-Ng, C., Mcclenahan, K., and Eamus, D. (2004). Convergence in hydraulic architecture, water relations and primary productivity amongst habitats and across seasons in Sydney. *Funct. Plant Biol.* 31, 429–439. doi: 10.1071/FP03194

Maherali, H., Pockman, W. T., and Jackson, R. B. (2004). Adaptive variation in the vulnerability of woody plants to xylem cavitation. *Ecology* 85, 2184–2199. doi: 10.1890/02-0538

Mcdowell, N. G. (2011). Mechanisms Linking Drought, Hydraulics, Carbon Metabolism, and Vegetation Mortality. *Plant Physiol.* 155, 1051–1059. doi: 10.1104/pp.110.170704

Navarro, A., Portillo-Estrada, M., Arriga, N., Vanbeveren, S. P., and Ceulemans, R. (2018). Genotypic variation in transpiration of coppiced poplar during the third rotation of a short-rotation bio-energy culture. *Glob. Change Biol. Bioenergy.* 10, 592–607. doi: 10.1111/gcbb.12526

Oren, R., Sperry, J., Katul, G., Pataki, D., Ewers, B., Phillips, N., et al. (1999). Survey and synthesis of intra-and interspecific variation in stomatal sensitivity to vapour pressure deficit. *Plant Cell Environ.* 22, 1515–1526. doi: 10.1046/j.1365-3040.1999.00513.x

Pammenter, N. W., and Vander Willigen, C. (1998). A mathematical and statistical analysis of the curves illustrating vulnerability of xylem to cavitation. *Tree Physiol.* 18, 589–593. doi: 10.1093/treephys/18.8-9.589

Pockman, W. T., and Sperry, J. S. (2000). Vulnerability to xylem cavitation and the distribution of Sonoran Desert vegetation. *Am. J. Bot.* 87, 1287–1299. doi: 10.2307/2656722

Qu, X., Cao, B., Kang, J., Wang, X., Han, X., Jiang, W., et al. (2019). Fine-tuning stomatal movement through small signaling peptides. *Front. Plant Sci.* 10, 69. doi: 10.3389/fpls.2019.00069

R Development Core, T (2017). *A language and environment for statistical computing* (Vienna: The R Foundation for Statistical Computing).

Saliendra, N. Z., Sperry, J. S., and Comstock, J. P. (1995). Influence of leaf water status on stomatal response to humidity, hydraulic conductance, and soil drought in *Betula occidentalis*. *Planta* 196, 357–366. doi: 10.1007/BF00201396

Scholander, P. F., Bradstreet, E. D., Hemmingsen, E. A., and Hammel, H. T. (1965). Sap Pressure in Vascular Plants: Negative hydrostatic pressure can be measured in plants. *Science* 148, 339–346. doi: 10.1126/science.148.3668.339

Scoffoni, C., Albuquerque, C., Brodersen, C. R., Townes, S. V., John, G. P., Bartlett, M. K., et al. (2017). Outside-Xylem Vulnerability, Not Xylem Embolism, Controls Leaf Hydraulic Decline during Dehydration. *Plant Physiol.* 173, 1197–1210. doi: 10.1104/pp.16.01643

Sperry, J., and Saliendra, N. (1994). Intra-and inter-plant variation in xylem cavitation in Betula occidentalis. *Plant Cell Environ.* 17, 1233–1241. doi: 10.1111/j.1365-3040.1994.tb02021.x

Sperry, J. S., and Sullivan, J. E. (1992). Xylem embolism in response to freeze-thaw cycles and water stress in ring-porous, diffuse-porous, and conifer species. *Plant Physiol.* 100, 605–613. doi: 10.1104/pp.100.2.605

Sperry, J. S. (1995). "Limitations on stem water transport and their consequences", in *Plant stems. Physiology and functional morphology*. Ed. B. L. Gartner (San Diego: Academic Press), pp. 105–121.

Tardieu, F., and Simonneau, T. (1998). Variability among species of stomatal control under fluctuating soil water status and evaporative demand: modelling isohydric and anisohydric behaviours. *J. Exp. Bot.* 49, 419–432. doi: 10.1093/jxb/49.Special_Issue.419

Thomas, F. M., Arndt, S. K., Bruelheide, H., Foetzki, A., Gries, D., Huang, J., et al. (2000). Ecological basis for a sustainable management of the indigenous vegetation in a Central-Asian desert: presentation and first results. *J. Appl. Bot.* 74, 212–219.

Thomas, F. M., Foetzki, A., Gries, D., Bruelheide, H., Li, X. Y., Zeng, F. J., et al. (2008). Regulation of the water status in three co-occurring phreatophytes at the southern fringe of the Taklamakan Desert. *J. Plant Ecol.* 1, 227–235. doi: 10.1093/jpe/rtn023

Torres-Ruiz, J. M. (2020). Virtual issue on Plant hydraulics: update on the recent discoveries. *Physiol. Plant.* 168, 758–761. doi: 10.1111/ppl.13081

Tyree, M. T., and Sperry, J. S. (1988). Do woody plants operate near the point of catastrophic xylem dysfunction caused by dynamic water stress? : answers from a model. *Plant Physiol.* 88, 574–580. doi: 10.1104/pp.88.3.574

Volaire, F. (2018). A unified framework of plant adaptive strategies to drought: Crossing scales and disciplines. *Global Change Biol.* 24, 2929–2938. doi: 10.1111/gcb.14062

Way, D. A., Domec, J. C., and Jackson, R. B. (2013). Elevated growth temperatures alter hydraulic characteristics in trembling aspen (Populus tremuloides) seedlings: implications for tree drought tolerance. *Plant Cell Environ.* 36, 103–115. doi: 10.1111/j.1365-3040.2012.02557.x

Wheeler, J. K., Huggett, B. A., Tofte, A. N., Rockwell, F. E., and Holbrook, N. M. (2013). Cutting xylem under tension or supersaturated with gas can generate PLC and the appearance of rapid recovery from embolism. *Plant Cell Environ.* 36, 1938–1949. doi: 10.1111/pce.12139

Woodruff, D. R., Mcculloh, K. A., Warren, J. M., Meinzer, F. C., and Lachenbruch, B. (2007). Impacts of tree height on leaf hydraulic architecture and stomatal control in Douglas-fir. *Plant Cell Environ.* 30, 559–569. doi: 10.1111/j.1365-3040.2007.01652.x

Wu, J., Zhang, X., Deng, C., Liu, G., and Li, H. (2010). Characteristics and dynamics analysis of Populus euphratica populations in the middle reaches of Tarim River. *J. Arid. Land.* 2, 250–256. doi: 10.3724/SP.J.1148.2010.00242

Yu, T., Feng, Q., Si, J., and Pinkard, E. A. (2019). Coordination of stomatal control and stem water storage on plant water use in desert riparian trees. *Trees* 33, 1–15. doi: 10.1007/s00468-019-01816-7

Zhang, Y. J., Rockwell, F. E., Graham, A. C., Alexander, T., and Holbrook, N. M. (2016). Reversible Leaf Xylem Collapse: A Potential "Circuit Breaker" against Cavitation. *Plant Physiol.* 172, 2261–2274. doi: 10.1104/pp.16.01191

Zhou, H., Chen, Y., Li, W., and Ayup, M. (2013). Xylem hydraulic conductivity and embolism in riparian plants and their responses to drought stress in desert of Northwest China. *Ecohydrology* 6, 984–993. doi: 10.1002/eco.1412

Zhou, X. (1993). "Features of the deserts and changes in the desert surrounding in Xinjiang," in *Desertification Control of Blown Sand Disasters in Xinjiang* (Beijing: Science Press), 1–63.

Conflict of Interest: The authors declare that the research was conducted in the absence of any commercial or financial relationships that could be construed as a potential conflict of interest.